



# Fe(III)-porphyrin heterogenized on MCM-41: Matrix effects on the oxidation of 1,4-pentanediol

Alessandra Molinari<sup>a</sup>, Andrea Maldotti<sup>a,\*</sup>, Amra Bratovic<sup>a</sup>, Giuliana Magnacca<sup>b</sup>

<sup>a</sup> Dipartimento di Chimica, Via Luigi Borsari 46, Università di Ferrara, 44100 Ferrara, Italy

<sup>b</sup> Dipartimento di Chimica Inorganica, Chimica Fisica, Chimica dei Materiali, Università di Torino, Via P. Giuria 7, 10125 Torino, Italy

## ARTICLE INFO

### Keywords:

Heterogeneous photocatalysis  
Iron porphyrins  
Diol oxidation  
MCM-41

## ABSTRACT

The metal complex iron *meso*-tetrakis(2,6-dichlorophenyl)porphyrin (Fe<sup>III</sup>P) has been covalently linked on the surface of the mesoporous material MCM-41 and of amorphous SiO<sub>2</sub> to give the photocatalysts Fe<sup>III</sup>P/MCM-41 and Fe<sup>III</sup>P/SiO<sub>2</sub> respectively. The effect of porphyrin addition on specific surface area and porosity of these materials has been evaluated by means of BET and BJH model applied to N<sub>2</sub> adsorption/desorption isotherms. It is seen that the MCM-41 sample presents the largest modification due to the presence of porphyrin: the pore size changes in average value and distribution, the pores formed in the presence of porphyrin being smaller and presenting a larger distribution.

The photochemical characterization of Fe<sup>III</sup>P/MCM-41 reveals that this is a robust photocatalyst able to induce the O<sub>2</sub>-assisted oxidation of 1,4-pentanediol. In particular, photoexcitation of Fe<sup>III</sup>P/MCM-41 causes the conversion of 1,4-pentanediol to the aldehyde derivative compound with 70% regioselectivity. It is noteworthy that this product can be accumulated with no formation of further oxidized compounds. Due to its high specific surface area, which guarantees a good dispersion of the active centres, Fe<sup>III</sup>P/MCM-41 is about four times more efficient than Fe<sup>III</sup>P/SiO<sub>2</sub>. Moreover, the nature of the support controls the regioselectivity of the photocatalytic process: this is due to both uptake phenomena and steric effects, which can control the approach of the diol to the photoactive iron porphyrin.

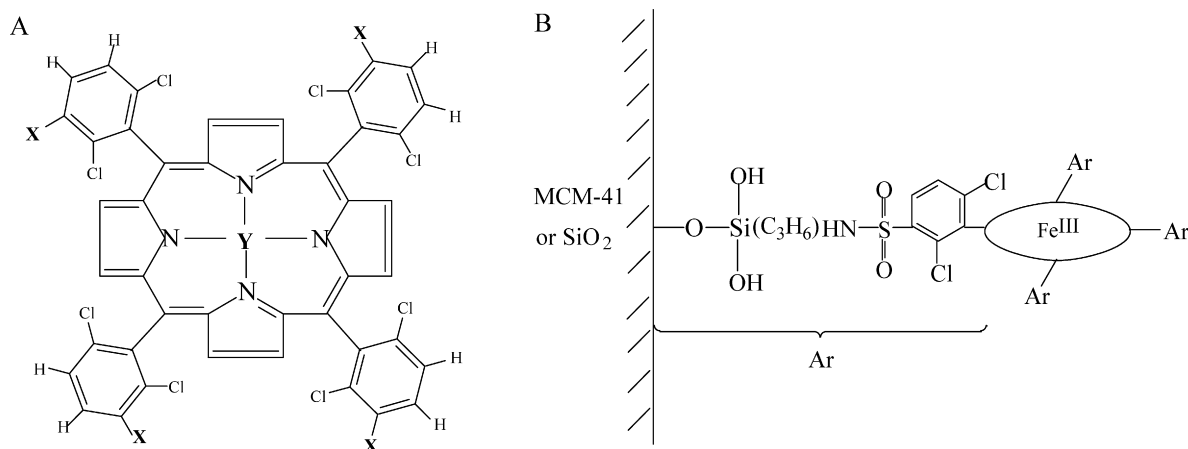
© 2010 Elsevier B.V. All rights reserved.

## 1. Introduction

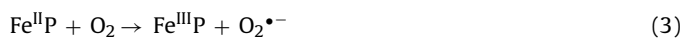
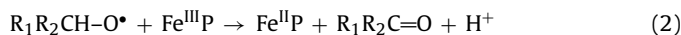
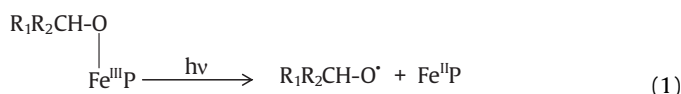
Molecular modification of solid support surfaces for the development of functional catalytic materials is a research field of high interest in heterogeneous catalysis. Among the inorganic supports, the use of mesoporous MCM-41 type silica has attracted much attention in the last years [1–5]. This material consists of uniform and hexagonal arrays of mesopores [6] and shows a high surface area. Even though different transition-metal complexes have been entrapped in molecular sieves, the major interest has been focused on metal complexes with oxidation-resistant aromatic ligands such as phthalocyanines, polypyridines and metalloporphyrins [7–13]. As a part of our ongoing interest in the preparation and characterization of heterogeneous photoactive systems for potential applications in oxidative catalysis [14], we have previously reported that MCM-41 can be successfully employed for supporting the polyoxoanion W<sub>10</sub>O<sub>32</sub><sup>4-</sup> [15].

Within this framework, we describe here the preparation and characterization of a new photocatalyst, based on the use of an iron porphyrin that has been covalently linked to the solid surface of MCM-41 (Fe<sup>III</sup>P/MCM-41). It is well-established that iron porphyrin complexes are able to induce the photocatalytic oxidation of primary and secondary alcohols in homogeneous solution according to the mechanism described by Eqs. (1)–(3) [14,16,17]. More specifically, irradiation in LMCT bands ( $\lambda = 300\text{--}400\text{ nm}$ ) of the Fe<sup>III</sup>porphyrin (Fe<sup>III</sup>P) in the presence of a primary or a secondary alcohol (R<sub>1</sub>R<sub>2</sub>CHOH, where R<sub>1</sub> = alkyl chain and R<sub>2</sub> = alkyl chain or H) induces the homolytic cleavage of the bond between Fe<sup>III</sup> and the axially coordinated alkoxide ion. This process causes oxidation and detachment of an alkoxide radical which may undergo further oxidation by Fe<sup>III</sup>P yielding the corresponding carbonylic derivative (Eq. (2)). The starting Fe<sup>III</sup>P can be regenerated as a consequence of the very fast reaction of the ferrous complex with molecular oxygen (Eq. (3)). The iron porphyrin here employed is the iron *meso*-tetrakis(2,6-dichlorophenyl)porphyrin (see Scheme 1A) bearing an aminopropylsilane chain that can be grafted on the surface of the mesoporous material. An interesting peculiarity of this complex is that the chlorine atoms present in the *meso*-aryl groups provide a steric protection of the porphyrin ring against its radical induced oxidative degradation [1].

\* Corresponding author. Tel.: +39 0532455147; fax: +39 0532240709.  
E-mail address: [mla@unife.it](mailto:mla@unife.it) (A. Maldotti).



**Scheme 1.** (A) Synthesis of the iron porphyrin complex bearing trifluorosilyl functions. (1) Y = 2H<sup>+</sup>, X = H; (2) Y = 2H<sup>+</sup>, X = SO<sub>2</sub>Cl; (3) Y = 2H<sup>+</sup>, X = SO<sub>3</sub>H; (4) Y = Fe<sup>3+</sup>, X = SO<sub>3</sub>H; (5) Y = Fe<sup>3+</sup>, X = SO<sub>2</sub>Cl; (6) Y = Fe<sup>3+</sup>, X = SO<sub>2</sub>NH(CH<sub>2</sub>)<sub>3</sub>Si(OEt)<sub>3</sub>; (7) Y = Fe<sup>3+</sup>, X = SO<sub>2</sub>NH(CH<sub>2</sub>)<sub>3</sub>SiF<sub>3</sub>. (B) Schematic representation of Fe<sup>III</sup>P/MCM-41 structure.



The Fe<sup>III</sup>P/MCM-41 material is studied in detail in this paper and the results of its chemico-physical characterization (specific surface area and porosity) are presented. Moreover, we assess its photocatalytic activity evaluating the regioselectivity in the oxidation of a multifunctional molecule such as 1,4-pentanediol in the presence of molecular oxygen. It is to be underlined that the selective oxidation of one of the alcoholic functionalities present in diols, with production of hydroxyaldehydes or hydroxyketones as the main products, is an important transformation in fine chemistry. The Fe<sup>III</sup>P/MCM-41 material is also compared with an analogous one where the same Fe<sup>III</sup>porphyrin complex is grafted on amorphous silica surface (Fe<sup>III</sup>P/SiO<sub>2</sub>): this should evidence the effect of the matrix on the photocatalyst activity.

## 2. Experimental

### 2.1. Catalyst preparation

The synthesis of the photocatalyst has been carried out following a procedure reported in a previous paper where the same Fe<sup>III</sup>porphyrin was linked on TiO<sub>2</sub> [18]. The porphyrin ring free base (1) in Scheme 1A was prepared following the known method reported by Lindsey et al. [19,20], using 2,6-dichlorobenzaldehyde and pyrrole as starting reagents. The subsequent steps for the preparation of the silanized iron porphyrin reported in Scheme 1A are briefly described in the following. An aromatic electrophilic substitution reaction with ClSO<sub>3</sub>H on (1) under rigorously controlled conditions (100 °C, 3 h) gave (2), which has been characterized by <sup>1</sup>H NMR [δ = 8.62 (s, 8H, H-pyrrole), δ = 8.60 (4H, H-*m*-phenyl), δ = 8.05 (4H, H-*p*-phenyl), δ = -2.51 (s, 2H, NH) in CDCl<sub>3</sub>, Varian Gemini 300 MHz]. Subsequent hydrolysis yielded (3) (IR stretching frequencies of SO<sub>3</sub>H groups are observed at 1190 and 1050 cm<sup>-1</sup>). Then, an aqueous solution of FeCl<sub>2</sub>·4H<sub>2</sub>O was allowed to react with (3) under argon at 80 °C for 18 h to give the iron porphyrin complex (4) (Soret band at 394 nm). After oxygenation of the sample, a solution of KOH (35%, all the percentages here presented correspond to percentage in weight of aqueous solutions) was added until pH 8–9 to precipitate iron

in excess as Fe(OH)<sub>3</sub>. After filtration, the reaction mixture was neutralized with HCl (35%) and the iron porphyrin complex was purified by column chromatography, concentrated and precipitated from acetone. Chlorination on complex (4) was performed (1 g) using PCl<sub>5</sub> (3.5 g) and POCl<sub>3</sub> (10 ml) at 50 °C, for 30 min leading to (5). This was a suitable complex for the nucleophilic substitution by excess of aminopropyl triethoxysilane (aptès, 160 mg/50 mg of (5)), for 17 h under argon at 70 °C in the presence of pyridine (30 μl) in THF (4 ml). The monomer (6) was obtained, dried in a rotary evaporator and the solid obtained was washed with aliquots of H<sub>2</sub>O/acetone/MeOH mixture. Then, it was recovered and dried in the oven. Solid monomer (6) was treated with HF (48%)/H<sub>2</sub>SO<sub>4</sub> (98%) 1:1 (6 ml/100 mg of complex (6)): the reaction mixture was left in rest for 30 min to produce the porphyrinotrifluorosilane monomer (7). Addition of CH<sub>2</sub>Cl<sub>2</sub> allowed the extraction of monomer (7) in the organic phase, while the excess of aptès, converted to aminopropyltrifluorosilane, remained in the aqueous acid solution. CH<sub>2</sub>Cl<sub>2</sub> solution containing (7) was washed several times using aliquots of aqueous solution of HF 20%, then methanol (25 ml) and 2,3-dimethoxypropane (10 ml) were added. After some hours of rest the solution was concentrated to a final volume of 20 ml: the UV–vis spectrum of the obtained solution (Soret band at λ<sub>max</sub> = 418 nm) was similar to that of the parent porphyrin (5), indicating that the porphyrin ring was not modified during the preparation.

Functionalization of MCM-41 with complex (7) to prepare the Fe<sup>III</sup>P/MCM-41 system has been accomplished as described in the following. MCM-41 (0.1 g) was suspended in the solution containing complex (7) (2 × 10<sup>-4</sup> M, 3 ml). The suspension was stirred in the dark for 20 min, then the coloured MCM-41 was recovered by centrifugation and dried at 80 °C. The amount of complex linked to the support was evaluated recording UV–vis spectra of the solution before and after the contact with MCM-41. An analogous procedure was followed to prepare Fe<sup>III</sup>P/SiO<sub>2</sub>, suspending 0.1 g of amorphous silica in 3 ml of the above solution of complex (7). In both cases, the contact between porphyrinotrifluorosilane monomer (7) and the silanols of the support leads to the breaking of Si–F bond and to the formation of a Si–O covalent bond: as a result, the iron porphyrin complex is covalently linked on the surface of the silica matrix, as shown in Scheme 1B.

### 2.2. Photocatalyst characterization

Diffuse reflectance UV–vis spectra were recorded with a Jasco V-570 using an integrating sphere and BaSO<sub>4</sub> as reference. The plot-

**Table 1**  
BET specific surface areas and porosity details of pure and modified supports.

Samples	BET specific surface area (m <sup>2</sup> /g)	BJH total porosity (cm <sup>3</sup> /g)	BJH pore size (determined on maximum) (Å)
MCM-41	960	0.73	25
Fe <sup>III</sup> P/MCM-41	826	0.71	23
SiO <sub>2</sub>	97	0.44	~100
Fe <sup>III</sup> P/SiO <sub>2</sub>	93	0.41	~100

ted spectra were obtained by the Kubelka–Munk transformation ( $F(R) = 1 - R^2/2R$ ) versus the wavelength. N<sub>2</sub> adsorption/desorption experiments were carried out at 77 K by means of ASAP2020 instrument (Micromeritics).

Adsorption experiments of the mono-alcohols (1-pentanol and 2-pentanol) were carried out suspending Fe<sup>III</sup>P/MCM-41 or Fe<sup>III</sup>P/SiO<sub>2</sub> (33 g/l) in 300 μL of CH<sub>3</sub>CN solutions containing increasing concentrations of both alcohols and keeping in the dark for 20 min under magnetic stirring. The amounts of adsorbed alcohols were obtained by GC analysis evaluating their concentration decrease in the solution. For sensitivity reason, we carried out these experiments reducing the volume of alcoholic solution and increasing the amount of solid sample in respect to the photocatalytic experiments.

### 2.3. Photocatalytic experiments

Photocatalytic experiments were carried out inside a closed Pyrex tube of 15 ml capacity at 298 ± 1 K joined through an inlet tube to a balloon filled with O<sub>2</sub>. Fe<sup>III</sup>P/MCM-41 or Fe<sup>III</sup>P/SiO<sub>2</sub> (4.5 g/l) was dispersed in 3 ml of a CH<sub>3</sub>CN solution containing 1,4-pentanediol (3% as volume percentage v/v) and stirred (120 min) to reach equilibrium conditions before irradiation. Photochemical excitation was performed irradiating the sample in the pyrex tube with an external Helios Q400 Italquartz medium-pressure Hg lamp, selecting wavelengths higher than 350 nm with a cut-off filter. The photon flux, measured with a MACAM UV203X ultraviolet radiometer, was 15 mW/cm<sup>2</sup>. At the end of the photocatalytic experiment, the sample was centrifuged, the products that remained adsorbed on the irradiated powders were extracted with CH<sub>2</sub>Cl<sub>2</sub> (2 times with aliquots of 3 ml each), and the organic phases were analyzed by GC. Products analyses were carried out by using a HP 6890 gas chromatograph, equipped with a flame ionisation detector and a DB-WAX capillary column. Quantitative analyses were performed with calibration curves obtained with standard samples. Each experiment was repeated three times in order to evaluate the error, which remained in the ±5% interval around mean values. Homogeneous reactions were carried out dissolving the iron porphyrin (Fe<sup>III</sup>(**1**), 2 × 10<sup>-5</sup> M) obtained through metallation of compound (**1**) of Scheme 1A in mixtures of CH<sub>3</sub>CN and 1,4-pentanediol (3%, v/v). Unfortunately, photocatalytic experiments were impossible to carry out because of the formation of a precipitate involving the iron porphyrin complex.

No oxidation products were obtained when blank experiments were run in the dark or irradiating in the absence of photocatalyst. Other experiments were carried out in order to test the stability of Fe<sup>III</sup>P/MCM-41 system: after the first run the photocatalyst was recovered, washed with CH<sub>2</sub>Cl<sub>2</sub> and CH<sub>3</sub>CN, dried at 80 °C for 1 h and then reused in a new experiment. This procedure has been repeated up to five cycles.

## 3. Results and discussion

### 3.1. Textural characterization

In the Fe<sup>III</sup>P/MCM-41 and Fe<sup>III</sup>P/SiO<sub>2</sub> prepared materials, the iron porphyrin complex is covalently linked on the surface of the support, as schematized in Scheme 1B. The loading of Fe<sup>III</sup>P on

the support corresponds to ~1% (w/w). The diffuse reflectance UV–vis spectra of Fe<sup>III</sup>P/MCM-41 and of Fe<sup>III</sup>P/SiO<sub>2</sub> indicate that the structure of the porphyrin remains unchanged during the immobilization procedure (see Supplementary Data).

The effect of porphyrin addition on specific surface area and porosity of Fe<sup>III</sup>P/MCM-41 and of Fe<sup>III</sup>P/SiO<sub>2</sub> has been evaluated by means of BET [21] and BJH [22] model applied to N<sub>2</sub> adsorption/desorption isotherms carried out at 77 K. The results summarized in Table 1 show that the specific surface area decreases for both samples in the presence of the iron porphyrin, but the change is much more relevant in the MCM-41 case. At the same time, for both supports, the presence of the iron porphyrin decreases the total porosity in a very limited extent.

In order to evaluate better the modification of the samples induced by the Fe<sup>III</sup>-porphyrin presence, it is useful to examine Figs. 1 and 2, which report the shape of the isotherms and the curves relative to pore size distribution respectively. It appears clearly that the MCM-41 sample presents a significant modification due to the presence of porphyrin. More specifically, the isotherm shape typical of a MCM-41 material (Fig. 1, solid-line curve) results modified (Fig. 1, circle-symbol curve): the first capillary condensation, typically narrow and present at  $p/p^0 = 0.35$  for unmodified MCM sample, moves downwards and it is accompanied by another not so evident capillary condensation (indicated in the figure by an arrow) which covers up to  $p/p^0 = 0.65$ , indicating a modification in the very regular mesoporous structure of MCM sample. Moreover, the porphyrin-containing material shows a small hysteresis loop associated to this capillary condensation (the hysteresis loop is evidenced in the figure by an arrow and closes at  $p/p^0 = 0.42$ , in agreement with what expected for the tensile strength of N<sub>2</sub> used as adsorptive gas). This indicates a modification in the pore shape with respect to what observed for unmodified MCM-41. In fact, the presence of a hysteresis loop is compatible with ink-bottle-like pores; i.e., pores characterized by cavities with a small access. A last capillary condensation (and corresponding hysteresis loop) is present at very high values of relative pressure ( $p/p^0 > 0.90$ ), indicating the possible presence of large mesoporosity, probably induced by inter-particle spaces due to particle aggregation, but this feature seems to be not affected by the presence of the porphyrin, so it will be not considered anymore.

No analogous modification is evidenced by isotherms relative to SiO<sub>2</sub> samples with or without porphyrin (see Supplementary Data). The curves are those typical of an almost not porous system (an hysteresis loop is visible in the range of relative pressure 0.75–1 but it is probably caused by particle aggregation, as mentioned above for MCM samples) and no visible changes are induced by porphyrin presence.

In order to confirm the consideration made above, the BJH model has been applied to adsorption branch and the following can be attained (compare Table 1 and Fig. 2). Total mesoporosity decreases slightly in the case of Fe<sup>III</sup>P/MCM-41 compared to unmodified MCM material, but the pore size changes in average value and distribution, the pores formed in the presence of porphyrin being smaller and presenting a larger distribution. Again, no analogous modifications were evidenced in the case of SiO<sub>2</sub> systems (see Supplementary Data).

In conclusion, the morphological features of MCM-41 have been clearly changed by porphyrin presence. The modification of

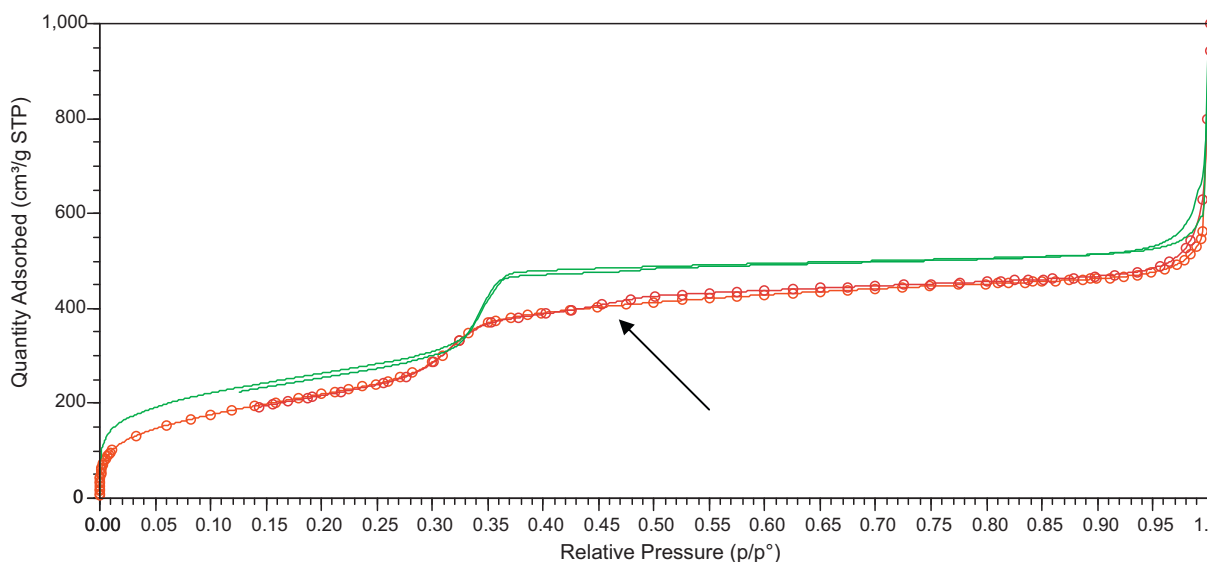


**Fig. 1.** Adsorption/desorption isotherms of  $N_2$  adsorbed at 77 K obtained for MCM-41 material: comparison between unfunctionalized sample (no symbols) and the functionalized one (circle symbols). The arrow indicates the presence of capillary condensation and corresponding hysteresis loop.

the porous texture may be explained considering that porphyrin molecules, when localized near a pore, likely cause a partial block of the cavity access. This renders slightly smaller and less accessible the mesopores of MCM material, giving reason of the specific surface area decrease and of the porous arrangement modification (different capillary condensation, presence of the hysteresis loop indicated by the arrow in Fig. 1). No analogous features can be deduced by  $N_2$ -gas-volumetric studies for  $SiO_2$  material, but in this case a much less ordered starting structure can induce a camouflage effect.

### 3.2. Photocatalytic oxidation of 1,4-pentandiol

The photocatalytic activity of  $Fe^{III}P/MCM-41$  has been assessed studying the oxidation of 1,4-pentandiol. Acetonitrile suspensions of this photocatalyst containing 1,4-pentandiol were irradiated ( $\lambda > 350$  nm) at room temperature and under 760 Torr of  $O_2$ . Photoexcitation caused the conversion of the diol to the products reported in Scheme 2: 4-hydroxypentanal (**a**) and 5-hydroxy-2-

pentanone (**b**) derive from the selective oxidation of primary or secondary hydroxy functional group of the diol. From chromatographic analysis, other two peaks were attributed to the cyclic emiacetalic diastereoisomers (**c**) derived from the closure of product (**a**). After 240 min irradiation, (**a**), (**b**) and (**c**) represented about the 95% of the overall gas chromatographic area of the detected products. No oxidation products were obtained when blank experiments were run in the absence of light or irradiating the dispersing medium without  $Fe^{III}P/MCM-41$ . From UV-vis spectra, no release of  $Fe^{III}$  porphyrin was detected during the photocatalytic experiment, thus confirming that we were in the presence of real heterogeneous catalytic processes. A loss of photocatalyst activity of about 30% in terms of detected products after irradiation was observed after five repeated cycles.

On the basis of the described results, we can state that the well known ability of photoexcited iron porphyrins to induce alcohol oxidation according to Eqs. (1)–(3) is retained also in the heterogeneous system  $Fe^{III}P/MCM-41$ . The nature of the photoproducts is consistent with the oxidation of one alcoholic functionality of the

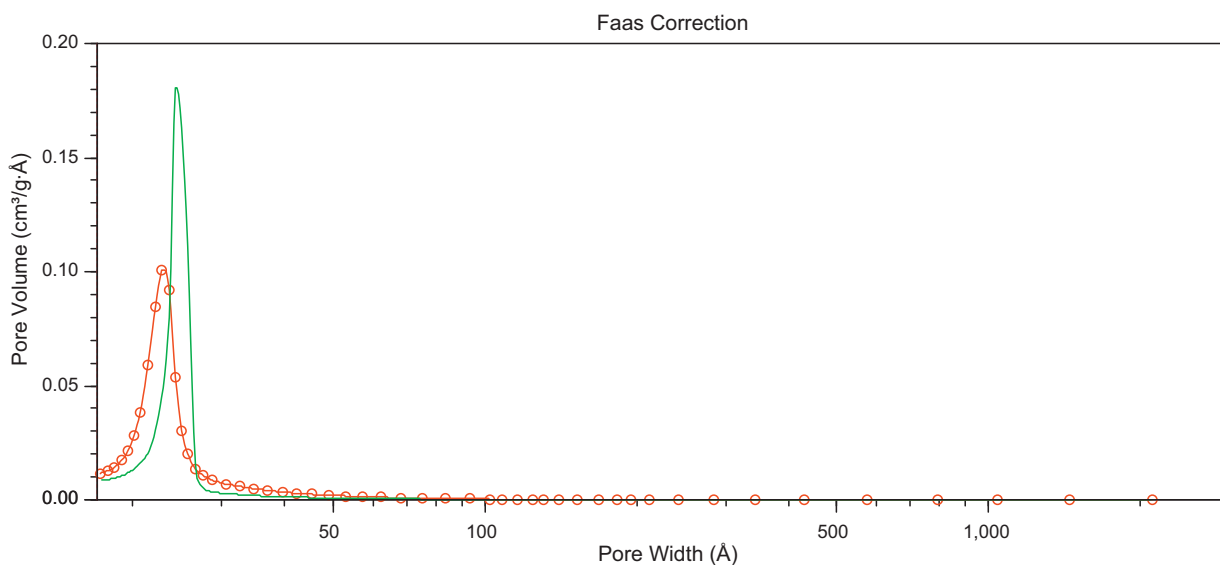
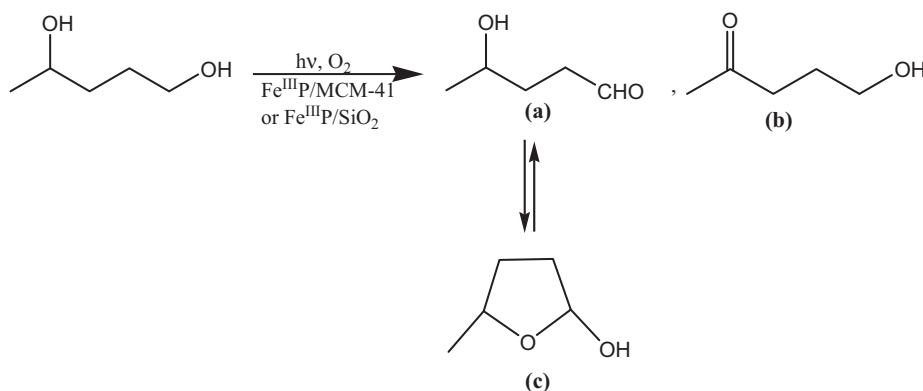


**Fig. 2.** BJH pore size distribution obtained from  $N_2$  adsorption at 77 K for MCM-41 sample: comparison between unfunctionalized sample (full line, no symbols) and the functionalized one (full line, circle symbols).



**Scheme 2.** Oxidized products obtained upon irradiation of  $\text{Fe}^{\text{III}}\text{P}/\text{MCM-41}$  or  $\text{Fe}^{\text{III}}\text{P}/\text{SiO}_2$  suspended in  $\text{CH}_3\text{CN}$  solutions containing 1,4-pentanediol in the presence of  $\text{O}_2$ .

diol, although two-site attack has been suggested as important in the oxidation of diols by the commonly employed electrochemical methods [23]. It is noteworthy that the partially oxidized products (a)–(c) can be accumulated with no formation of ketoacids.

The photocatalytic properties of  $\text{Fe}^{\text{III}}\text{P}/\text{MCM-41}$  in the oxidation of 1,4-pentanediol are summarized in Table 2 as  $\mu\text{moles}$  of aldehyde and its isomers ( $n(\mathbf{a} + \mathbf{c})$ ) and ketone ( $\mathbf{nb}$ ) obtained after 120 and 240 min irradiation. The concentration ratio between aldehyde and ketone (last column of Table 2) enables us to evaluate the regioselectivity of the photocatalytic process. It is seen that  $\text{Fe}^{\text{III}}\text{P}/\text{MCM-41}$  is able to photooxidize 1,4-pentanediol in 1-position with good selectivity, since the aldehyde to ketone concentration ratio is 2.4 after 240 min photoexcitation.

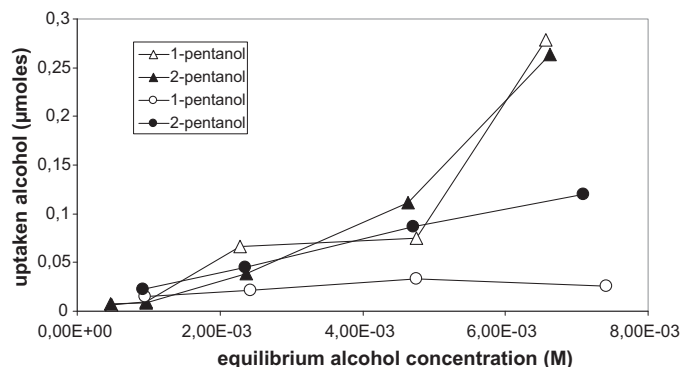
The photocatalytic activity of the iron porphyrin is significantly lower when it is bound on the surface of amorphous silica rather than on the mesoporous material. In fact, Table 2 indicates that the overall oxidation yield of 1,4-pentanediol to carbonylic compounds with  $\text{Fe}^{\text{III}}\text{P}/\text{MCM-41}$  is about four times higher than that obtained with  $\text{Fe}^{\text{III}}\text{P}/\text{SiO}_2$ . It is plausible that the mesoporous photocatalyst, with its very wide surface area, is able to disperse better the added amount of iron porphyrin, thus providing a greater number of photocatalytic sites and preventing the formation of photochemically inactive aggregates.

Table 2 shows that  $\text{Fe}^{\text{III}}\text{P}/\text{MCM-41}$  and  $\text{Fe}^{\text{III}}\text{P}/\text{SiO}_2$  differ also in terms of regioselectivity; in fact, the ketone (**b**) is the main product when the iron porphyrin is linked on the surface of amorphous silica. This difference may be due, at least in part, to surface phenomena that can control how diol molecule approaches to the photoactive iron porphyrin. Previous investigations on the photocatalytic oxidation of diols by titanium dioxide [24] or heterogenized polyoxotungstates [25] have demonstrated the important role played by uptake phenomena on the surface. For this reason, we carried out some experiments in order to evaluate the interaction strength of the two hydroxy functional groups of the diol with the solid surfaces of  $\text{Fe}^{\text{III}}\text{P}/\text{MCM-41}$  and  $\text{Fe}^{\text{III}}\text{P}/\text{SiO}_2$ . These

materials were suspended in  $\text{CH}_3\text{CN}$  mixtures containing both the monofunctional alcohols 1-pentanol and 2-pentanol, which simulate the two different hydroxy groups present in 1,4-pentanediol. We evaluated the uptake of these alcohols after 20 min of stirring. For sensitivity reason, we carried out these experiments reducing the volume of the alcoholic solutions employed and increasing the amount of solid samples with respect to the photocatalytic experiments. Fig. 3 shows that 2-pentanol interacts with  $\text{Fe}^{\text{III}}\text{P}/\text{SiO}_2$  in a greater extent than 1-pentanol (circles). This is an indication that also the secondary –OH functional group of 1,4-pentanediol undergoes a preferential interaction with the surface of  $\text{Fe}^{\text{III}}\text{P}/\text{SiO}_2$ , so explaining why the ketone (**b**) is the main product upon irradiation of  $\text{Fe}^{\text{III}}\text{P}/\text{SiO}_2$ .

Fig. 3 shows that the interaction strengths of 2-pentanol and 1-pentanol on  $\text{Fe}^{\text{III}}\text{P}/\text{MCM-41}$  are comparable (triangles), suggesting that in this case, besides uptake phenomena on the surface, other textural effects must be responsible of the observed ability of this material to convert preferentially 1,4-pentanediol to the corresponding hydroxyl–aldehyde (**a**). The physico-chemical characterization described above is compatible with a modification of the pore shape with respect to what observed for unmodified MCM-41 and with the formation of ink-bottle-like pores. The modification of the porous texture has been explained above considering that  $\text{Fe}^{\text{III}}$ -porphyrin molecules are mainly localized near the ordered mesopore entrance, creating some kind of channel narrowing. As a consequence, a sort of steric control may favour the preferential coordination and the subsequent oxidation of the primary hydroxy functional group of 1,4-pentanediol to give the aldehydic derivative.

As the last point of this discussion, we collected experimental evidences that  $\text{Fe}^{\text{III}}(\mathbf{1})$  complex can not be employed as it is for



**Fig. 3.** Uptake of 1-pentanol (empty symbols) and 2-pentanol (full symbols) on  $\text{Fe}^{\text{III}}\text{P}/\text{SiO}_2$  (circles) and on  $\text{Fe}^{\text{III}}\text{P}/\text{MCM-41}$  (triangles).  $\text{Fe}^{\text{III}}\text{P}/\text{SiO}_2$  or  $\text{Fe}^{\text{III}}\text{P}/\text{MCM-41}$  (33 g/l) were suspended in 0.3 ml of  $\text{CH}_3\text{CN}$  containing increasing amounts of the two alcohols.

**Table 2**

Photocatalytic properties<sup>a</sup> of  $\text{Fe}^{\text{III}}\text{P}/\text{MCM-41}$  and  $\text{Fe}^{\text{III}}\text{P}/\text{SiO}_2$  in the oxidation of 1,4-pentanediol.

Photocatalyst	$n(\mathbf{a} + \mathbf{c})^b$	$\mathbf{nb}^b$	$n(\mathbf{a} + \mathbf{c})/\mathbf{nb}$
$\text{Fe}^{\text{III}}\text{P}/\text{MCM-41}$ , 120 min	2.6	1.5	1.7
$\text{Fe}^{\text{III}}\text{P}/\text{MCM-41}$ , 240 min	5.1	2.1	2.4
$\text{Fe}^{\text{III}}\text{P}/\text{SiO}_2$ , 120 min	0.3	0.7	0.4
$\text{Fe}^{\text{III}}\text{P}/\text{SiO}_2$ , 240 min	0.3	1.6	0.2

<sup>a</sup> In a typical experiment the employed photocatalyst (4.5 g/l) was suspended in a  $\text{CH}_3\text{CN}$  solution (3 ml) containing 1,4-pentanediol (3%, v/v) and irradiated ( $\lambda > 350$  nm) at  $298 \pm 1$  K and 760 Torr of  $\text{O}_2$ . Reported values are the mean of three repeated experiments (error =  $\pm 5\%$ ).

<sup>b</sup> Amount of carbonylic compounds as  $\mu\text{moles}$  obtained in 3 ml of solution.

the photocatalytic oxidation of 1,4-pentanediol in homogeneous solution. In fact, dissolution of Fe<sup>III</sup>(1) in mixtures of CH<sub>3</sub>CN and diol led to the formation of a precipitate with a concomitant decay in absorbance in all the UV–vis spectrum. We believe that the bifunctional character of diol favours the formation of insoluble 1,4-pentanediol-bridged Fe<sup>III</sup>(1) oligomers (in fact, no spectral changes and no precipitate were observed when Fe<sup>III</sup>(1) was dissolved in pure CH<sub>3</sub>CN) and this provokes a loss of the active molecules. This problem does not occur when the photoactive component is covalently bonded to the support of the heterogeneous catalyst.

#### 4. Conclusions

A silanized Fe<sup>III</sup> porphyrin has been linked on the mesoporous material MCM-41 for the first time. The presence of the iron porphyrin causes significant modifications of the MCM-41 porosity, in that the pores formed in the presence of the metal complex are smaller and present a larger distribution. More specifically, the iron porphyrin complex, when localized near a pore, seems to cause a partial block of the cavity access. No analogous feature can be deduced for the SiO<sub>2</sub> material Fe<sup>III</sup>P/SiO<sub>2</sub>.

The photochemical characterization of Fe<sup>III</sup>P/MCM-41 reveals that this is a robust photocatalyst able to induce the O<sub>2</sub>-assisted oxidation of 1,4-pentanediol. In particular, photoexcitation of Fe<sup>III</sup>P/MCM-41 causes the conversion of the 1,4-pentanediol to the aldehyde derivative with good regioselectivity. It is noteworthy that this partially oxidized product can be accumulated with no formation of further oxidized compounds. The oxidation rate of 1,4-pentanediol with Fe<sup>III</sup>P/MCM-41 is about four times higher than that obtained with Fe<sup>III</sup>P/SiO<sub>2</sub>, likely because the high surface area of the mesoporous material allows a better dispersion of the iron porphyrin. The nature of the support also controls the regioselectivity of the photocatalytic process: this may be due both to uptake phenomena, which can control how the diol approaches to the photoactive iron porphyrin and to some kind of steric control that may favour the preferential coordination and the subsequent oxidation of the primary hydroxy functional group of 1,4-pentanediol. It is to be underlined that the Fe<sup>III</sup>(1) complex can be employed for the photocatalytic oxidation of 1,4-pentanediol only after its heterogenization with MCM-41 or SiO<sub>2</sub>. In fact, the formation of inactive 1,4-pentanediol-bridged Fe<sup>III</sup>(1) oligomers occurs in homogeneous solution.

The results reported in this work provide new insights into the role of textural effects on the photocatalytic properties of iron porphyrins supported on solid matrices. This work is an additional example of how the study of the morphology and of the surface properties of functional materials is a fundamental point for developing efficient, selective and robust photocatalytic systems.

#### Appendix A. Supplementary data

Supplementary data associated with this article can be found, in the online version, at doi:10.1016/j.cattod.2010.09.004.

#### References

- [1] L. Washmon-Kriel, V.L. Jimenez, K.J. Balkus jr., *J. Mol. Catal. B: Enzym.* 10 (2000) 453–469.
- [2] R.Y.V. Subba, D.E. De Vos, P.A. Jacobs, *Angew. Chem. Int. Ed. Engl.* 36 (1997) 2661–2663.
- [3] S. Jun, R. Ryoo, *J. Catal.* 195 (2000) 237–243.
- [4] A. Martiez, G. Prieto, *Top. Catal.* 52 (2009) 75–90.
- [5] A. Fuerte, A. Corma, M. Iglesias, E. Morales, F. Sanches, *J. Mol. Catal. A: Chem.* 246 (2006) 109–117.
- [6] C.T. Kresge, M.E. Leonowicz, W.J. Roth, J.C. Vartulli, J.S. Beck, *Nature* 359 (1992) 710–712.
- [7] R.F. Parton, I.F.J. Vankelecom, M.J.A. Casselman, C.P. Bezonkhanova, J.B. Uytterhoeven, P.A. Jacobs, *Nature* 370 (1994) 541–544.
- [8] S.B. Ogunwumi, T. Bein, *J. Chem. Soc. Chem. Commun.* (1997) 901–902.
- [9] M.J. Sabater, A. Corma, A. Domenech, V. Fornes, H. Garcia, *J. Chem. Soc. Chem. Commun.* (1997) 1285–1286.
- [10] B.Z. Zhan, X.Y. Li, *Chem. Commun.* (1998) 349–350.
- [11] J.-L. Zhang, Y.-L. Liu, C.-M. Che, *Chem. Commun.* 23 (2002) 2906–2907.
- [12] M. Pal, V. Ganesan, *Langmuir* 25 (2009) 13264–13272.
- [13] A. Hamza, D. Srinivas, *Catal. Lett.* 128 (2009) 434–442.
- [14] A. Maldotti, A. Molinari, R. Amadelli, *Chem. Rev.* 102 (2002) 3811–3836.
- [15] A. Maldotti, A. Molinari, G. Varani, M. Lenarda, L. Storaro, F. Bigi, R. Maggi, A. Mazzacani, G. Sartori, *J. Catal.* 209 (2002) 210–216.
- [16] C. Bartocci, A. Maldotti, G. Varani, P. Battioni, V. Carassiti, D. Mansuy, *Inorg. Chem.* 30 (1991) 1255–1259.
- [17] A. Maldotti, A. Molinari, I. Vitali, E. Ganzaroli, P. Battioni, D. Mathieu, D. Mansuy, *Eur. J. Inorg. Chem.* (2004) 3127–3135.
- [18] A. Molinari, R. Amadelli, L. Antolini, A. Maldotti, P. Battioni, D. Mansuy, *J. Mol. Catal. A: Chem.* 158 (2000) 521–531.
- [19] T.G. Traylor, S. Tshuchiva, *Inorg. Chem.* 26 (1987) 1338–1339.
- [20] J.S. Lindsey, H.C. Hsu, I.C. Schreiman, *Tetrahedron Lett.* 27 (1986) 4969–4970.
- [21] S. Brunauer, P.H. Hemmet, E. Teller, *J. Am. Chem. Soc.* 60 (1938) 309–319.
- [22] E.P. Barrett, L.S. Joyner, P.P. Halenda, *J. Am. Chem. Soc.* 73 (1951) 373–380.
- [23] G. Horanyi, K. Torkos, *J. Electroanal. Chem.* 125 (1981) 105–113.
- [24] A. Molinari, M. Bruni, A. Maldotti, *J. Adv. Oxid. Technol.* 11 (2008) 143–150.
- [25] A. Maldotti, A. Molinari, F. Bigi, *J. Catal.* 253 (2008) 312–317.